Pak. J. Agri. Sci., Vol. 52(3), 845-852; 2015
ISSN (Print) 0552-9034, ISSN (Online) 2076-0906
http://www.pakjas.com.pk

NUMERICAL SIMULATION AND PARAMETERS OPTIMIZATION OF HEATED GLASS GREENHOUSE

Wu Feiqing[1,*], Xu Fang[2]and Zhang Libin[2]

[1]School of Information Science and Engineering, Ningbo Institute of Technology, Zhejiang University, Zhejiang Ningbo 315100, China, [2]The MOE Key Laboratory of Mechanical manufacture and Automation, Zhejiang University of Technology, Zhejiang Hangzhou 310014,China
[*]Corresponding author's e-mail: **wfq2006@yeah.net**

Although green house air heaters are often used throughout the southern Yangtze River basin in China, few data exist to indicate the proper placement of warm-air-delivery ducts, the arrangement of their air outlets, and the impact of thermal screens on the heated green houses environment. To better understand these issues, we develop herein a thermal-environment model of a Venlo-type glass green house on a winter night. The model is based on the standard $k-\varepsilon$ turbulence model, the buoyancy model, and the porous-medium model, and simulations based on this model are done by using commercial computational fluid dynamics software. The results indicate that the thermal distribution at the crop-canopy height significantly impacts crop growth and quality, so we used temperature distribution to evaluate the effect of the various heating parameters. We find that a higher average temperature and a greater temperature difference occur for downward vents than for horizontal vents. In addition, higher average temperature and smaller temperature difference occur for a thermal screen 3.6 m above the floor than for no thermal screen. Finally, we optimize the placement of the warm-air-delivery duct and the location of the outlet openings to obtain a more uniform thermal distribution and, thereby, better crop growth.
Keywords: Controlled crop environment, hot-air heating, computational fluid dynamics, numerical simulation, glass green house

INTRODUCTION

In most areas of China, cold winter nights make it necessary to supplement heating of green houses to ensure normal growth of green house crops. According to existing data, the ratio of fuel consumption to vegetable dry matter produced in green houses is five to one, and in some cases as it might even reach ten to one. This means that a lot of energy is wasted: only 40% to 50% of the energy is being used (Sheng, 2007). Thus, energy consumption due to green house heating in winter hinders the green house industry in China, and one of the most important factors leading to this high energy consumption is the non optimized arrangement of heating equipment within green houses.

In a green house, a heating system is an essential for the normal growth and development of green house crops in winter. The effect of different heating methods and strategies on green house performance has been investigated by many groups (Perdigones *et al*., 2006; Sethi and Bartzanas, 2007; Teitel *et al*., 1999; Meneses and Montero, 1990; Hoare and Morris, 1956). Teitel and Tanny (1998) and Kempkes *et al*. (2000) analyzed how the position of the heating system affects the vertical distribution of crop temperature and transpiration. The Takagi-Sugeno controller was designed to control nocturnal temperature in green houses by using air heating (Nachidi *et al.*, 2011). In other work, numerical simulations were developed to study green house heating (Willits *et al.*, 2004; Ghosal *et al.*, 2004).

The progress of computational fluid dynamics (CFD) technology has allowed simulations to be made of the environment within plastic-covered green houses, which are heated by using hot water (Zhu, 2005), and of the environment within Venlo-type glass green houses, which are heated by using air heaters (Sheng, 2007). Air heaters are generally used as the primary heating source for green houses in the winter in the southern area of the Yangtze River basin in China, which has a lower demand for energy. Although the temperature distribution in a green house, particularly at the crop-canopy level, significantly influences crop quality and overall production efficiency (Wang, 2004), data on air heating are insufficient. In particular, little information is available on the effect of the various heating parameters on the green house environment. We address these issues in this paper by first developing a CFD model of a green house environment and then, with the help of CFD software, analyzing how different parameters influence the green house environment. Finally, we optimize the relevant heating parameters to save energy.

MATERIALS AND METHOD

***Experimental green house*:** The simulated green house (Fig. 1) was located at the Zhejiang University of Technology (longitude 120° 10', latitude 30° 15'), was oriented north-

south, and was covered with 4-mm-thick superior float glass with a light transmittance of at least 85%. The green house was about 24 m long by 9.6 m wide by 4 m high (gutter height). At the northwest corner of the green house was an oil-fired air heater with a maximum power of 2.1×10^5 kJ/h, and a thermal screen and warm-air-delivery duct were installed under the roof to satisfy actual demand. A 22-m-long warm-air-delivery duct was fixed in the middle of the green house and ran from west to east, 2.4 m above the ground. The delivery duct was perforated with 300-mm-diameter holes separated by 1 m.

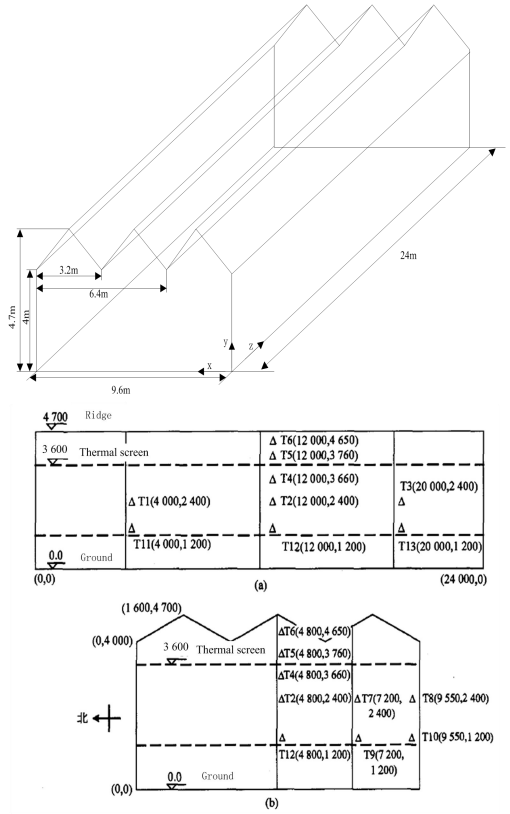

Figure 1. Sketch of simulation green house.

Model and computational conditions

1. *Basic control equation*: The classical mass, momentum, energy, and concentration equations are represented for a steady-state, three-dimensional flow by the following conservation equation (Wang, 2004):

$$\frac{\partial(\rho\phi)}{\partial t} + div(\rho\vec{u}\phi) = div(\Gamma\, grad\ \phi) + S\phi \qquad (1)$$

where ρ is the fluid density (kg/m^3), $\vec{u}$ is the velocity vector (m/s), and Γ and S_ϕ are the diffusion coefficient and source term, respectively. In Eq. (1), ϕ is a general variable: it could represent the velocity components, the temperature, etc.

2. *Turbulent model and buoyancy force model*: The flow of indoor air forced by an air heater is inevitably turbulent in a green house with border restrictions, so air flow is regarded as turbulent (Tao, 2004). Taking the turbulence model and computational accuracy into consideration, we adopted the standard $k-\varepsilon$ model (Wu, 2011).

Along the length of the delivery duct, hot wind was forced out of the holes in the duct, leading to natural convection in the internal air. Thus, in addition to forced convection, a buoyancy force exists because of the air-temperature difference (Tao, 2004). In this work, we used the Boussinesq assumption (Tong *et al.*, 2003) to account for the buoyancy force.

3. *Radiation model*: On winter nights, heat loss occurs by thermal radiation due to the higher indoor temperature. The discrete ordinates (DO) radiation model applies the radiative-transfer equation to a finite number of discrete solid angles, each associated with a vector direction fixed in the global Cartesian system. The DO model spans the entire range of optical thicknesses, which allows the user to tackle problems ranging from surface-to-surface radiation to participating radiation in combustion problems. The DO model can also be used to describe radiation at semitransparent walls (e.g., glass).

The DO model uses the radiative transfer equation (RTE) in the direction $\vec{s}$ as a field equation. The RTE for an absorbing, emitting, and scattering medium at position $\vec{r}$ and in the direction $\vec{s}$ is (Wu, 2011)

(2)

where is the position vector, is the direction vector, is the scattering-direction vector, is the path length, is the absorption coefficient, is the index of refraction, is the scattering coefficient, is the Stephan-Boltzmann constant, (W/m^2) is the radiation intensity, which is a function of position and direction , is the local temperature (K), is the phase function, is the solid angle (sr), and is the optical thickness or opacity of the medium. The index of refraction is important when considering radiation in semitransparent media.

4. *Crop model*: The porous-media model is designed to simulate the effect of crops on the air flow, which includes two parts: the first part is viscous loss (i.e., Darcy's law) and the second part is loss due to internal resistance. In addition, as part of the heating process, energy exchange (including sensible heat and latent heat) and mass exchange occur between air and crops. To consider the effect of crop drag and the energy exchange between air and crops, the source term is modified as follows (*Baille et al., 2006*):

, (3)

where is the energy source term (J), is the sensible-heat source term (J), and is the latent-heat source term (J).

The sensible-heat source term is given by

, (4)

where is the leaf-surface index (e.g., 2.6), is the specific heat of air at room temperature (kJ kg^{-1} K^{-1}), is the average crop temperature (K), is the indoor air temperature (e.g., average temperature 285.65 K), and is the aerodynamic drag of the crops. If internal air velocity were less than 0.1 m/s, , otherwise , where d is the characteristic blade length (6 mm) and u is the air velocity.

The latent-heat source term is given by

(5)

where is the latent heat of vaporization (K J/kg), is the relative humidity of the crops (83.4%), is the relative humidity of air (e.g., 80.3%), and is the stomatal resistance of the crops (s/m) and is given by

(640 s/m at night), where R_{gi} is the total internal sun radiation (W), and D_i is the difference in saturated-water-vapor pressure (Pa).

5. ***Computational domain and grid generation*****:** The simulated green house was symmetric about its central plane running lengthwise. Thus, to save storage space and improve computational efficiency, we used only half of the green house space as our three-dimensional computational domain. This had no effect on the accuracy of the results. In the model, the input and the output could be simplified to a velocity inlet and a semicircular outlet.

Generating the numerical mesh is a very important step in any numerical computation. For this work, using a mesh of equal-sized elements would be inappropriate because of the huge difference between the maximum and minimum sizes (a factor of 80). Therefore, the computational domain was divided into three subdomains with mesh sizes of 50, 150, and 300 mm (see Fig. 2). However, the ultimate accuracy and efficiency of any numerical calculation depends mainly on the mesh quality and the algorithm used. Considering the mesh continuity across the three subdomains and the irregular structure of a Venlo-type green house roof, we used nonstructural meshes to obtain mesh elements that varied in size. In addition, the mesh near the vents of the warm-air-delivery duct, the air outlet, and the crops were made smaller. The mesh near the inner wall was also made smaller to more accurately capture the huge temperature gradient across these walls.

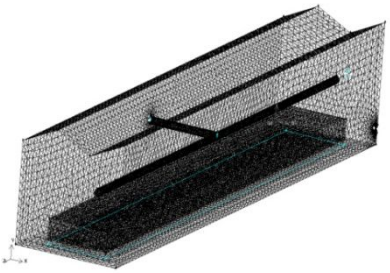

Figure 2. Computational domain mesh of CFD model for optimizing duct structure.

6. ***Boundary conditions*****:** After generating the mesh, we defined the boundaries of the computational domain. These included one velocity inlet, one pressure outlet, and a wall. In addition, the crop domain was defined as a porous medium, and other domains were defined as fluid.

The entire green house was defined as the computational domain because it is closed when heated. During heating, energy transfers between the indoor air and the wall, between the air and the crops, between hot and cold air, etc. The wall and the indoor air exchange energy by thermal convection, so we used the relevant coefficient of thermal conduction. The ground surface was defined as an adiabatic wall, and remaining boundary conditions were set according to measurements.

The parameters, such as the attributes of the wall and the air, and the initial boundary conditions of the green house are shown in Table 1. Because the outdoor temperature was more stable during the experiment, the outside temperature was fixed.

Table 1. Initial parameters and boundary conditions.

Parameter	Value	Units
Air density	1.225	kg/m^3
Thermal conductivity of air	0.0225	W m^{-1} K^{-1}
Thermal expansion coefficient of air	3.356×10^{-3}	K^{-1}
Specific heat of air (C_p)	1.005	kJ kg^{-1} K^{-1}
Air viscosity ( )	1.83×10^{-5}	kg m^{-1} s^{-1}
Glass density	2500	kg/m^3
Thermal conductivity of glass	0.74	W m^{-1} K^{-1}
Heat transfer coefficient of glass	6.4	W m^{-2} K^{-1}
Outer pressure (P)	10 1325	Pa
Duct inlet velocity ( )	6.0	m/s
Duct inlet temperature (T)	320	K
Outdoor temperature (T)	278	K
Crop pressure drop coefficient	0.395	

Crop internal loss factor	0.2

RESULTS

In the Fluent CFD simulation, we used the finite volume method (FVM). Discretization of the governing equations is illustrated most easily by considering the steady-state conservation equation for transport of a scalar quantity Φ. This is demonstrated by the following equation written in integral form for an arbitrary control volume V (Wang, 2004):

(6)

where is the density (kg/m^3), $\vec{v}$ is the velocity (m/s), $\vec{A}$ is the surface-area vector (m^2), Γ_ϕ is the diffusion coefficient for ϕ, $\nabla\phi$ is the gradient of ϕ, and S_ϕ is the source term for ϕ per unit volume.

We used FVM with the PISO algorithm to solve the differential equation (6) describing the flow field (we used PISO because it is more computationally efficient than the standard SIMPLE algorithm).

These models and boundary conditions were shown by Wu (2010) to be consistent with experiment. To accurately determine the air flow at the warm-air outlet and the temperature distribution, we used sections of (X = 3.2 m, Y = 2.4 m). Because crop growth depends on the environment, and in particular the distribution of the crop-canopy temperature, we used the section (Y = 1.2 m) to evaluate the heating parameters.

***1. Effect of warm-air outlet on temperature field*:**

***Effect of downward-directed warm-air outlet*:** Figure 3 shows the temperature distribution near the warm-air outlet. These results show that the ventilation gradually increases along the length of the warm-air duct, so the volume of warm air increases upon approaching the end of the duct. Also, more energy is exchanged with the internal air, so its temperature increases. The simulation shows that the warm air diffuses down primarily because of wind pressure. The energy continues to transfer to lower zones, exchanging energy with the indoor air, but warm air rises slowly with a slower diffusion velocity when buoyancy dominates (this is called the buoyancy effect). From Fig. 3, we see that the temperature below the duct is significantly higher than that above the duct, and at the crop-canopy level the temperature ranges from 290.15 to 304.75 K with an increased temperature difference of 14.6 K. In addition, the maximum temperature of nearly 305 K exceeds suitable crop temperatures (≤303.15K). Thus, considering crop growth, this environment is not suited for green house crops.

(a)

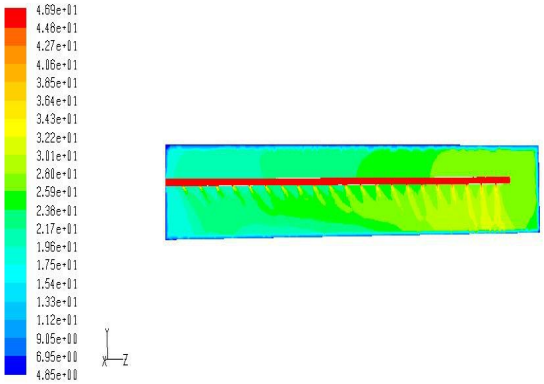

(b)

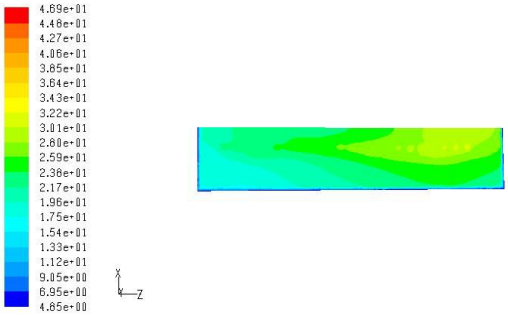

Figure 3. Temperature distribution in different sections. a) Temperature distribution in section (X = 3.2 m); b) Distribution of crop-canopy temperature in section (Y = 1.2 m).

***Effect of horizontally directed warm-air outlet*:** Figure 4 shows the temperature distribution near the horizontally directed warm-air outlet. The results show that the ventilation rate gradually increases upon increasing of the number of outlets along the duct. Adding more warm-air outlets increases the number of heat sources, resulting in more energy exchange within the indoor air. As a result, the internal temperature field is relatively uniform, and the warm-air volume follows more and more along the direction of the duct. At the end of the duct, the temperature is therefore higher. Except for the horizontal warm-air outlets, the buoyancy effect, and the lack of downward convection, less energy is exchanged in the lower green house zone, so there the temperature decreases overall, ranging from 288.15 to 296.95 K at the crop-canopy level with a temperature difference of 8.8 K. Compared with the downward-directed warm-air outlet, the temperature distribution tends to be reasonable and uniform at the crop-canopy level.

(a)

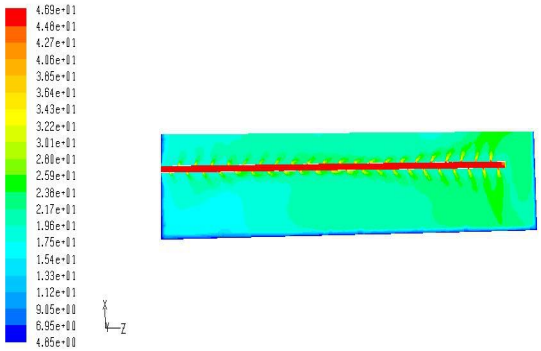

(b)

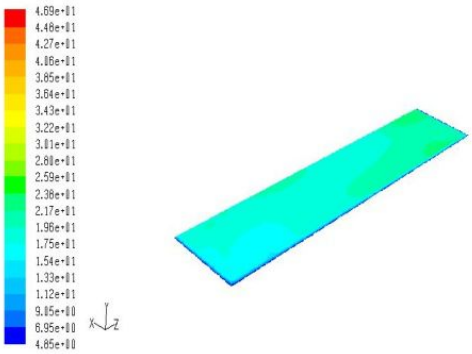

Figure 4. Temperature distribution in different sections. a) Temperature distribution in section (*Y* = 2.4 m); b) Distribution of crop-canopy temperature in section (*Y* = 1.2 m).

***Effect of optimization duct structure*:** Based on this analysis of the simulation results, we concluded that warm airflow varies greatly along the length of the duct, causing an unbalanced distribution in energy because of a large pressure gradient. To overcome this problem, we optimized the warm-air inlet of the duct by placing it at the center of the duct to reduce the flow length, which should reduce the pressure gradient. The temperature distribution for the optimized inlet and outlet is shown in Fig. 5(a).

The results of Fig. 5(a) show less change in ventilation from one end of the duct to the other and a more uniform temperature distribution, especially at the crop-canopy level [see Fig. 5(b)]. The optimized temperature ranges from 292.55 to 297.95 K at the crop-canopy level (difference of 5.4 K) and the maximum temperature difference is 3 K, which is across the *Z*-*Z* cross section at *X* = 4.8 m, *Y* = 1.2 m. Compared with the case of the horizontally directed warm-air outlet, the temperature at the crop canopy level is more even and is 4~5 K higher than the average temperature. This means that achieving the same temperature requires less energy than for the horizontally directed warm air outlet. Still, for the same green house structure, a thermal screen can be installed to save energy.

(a)

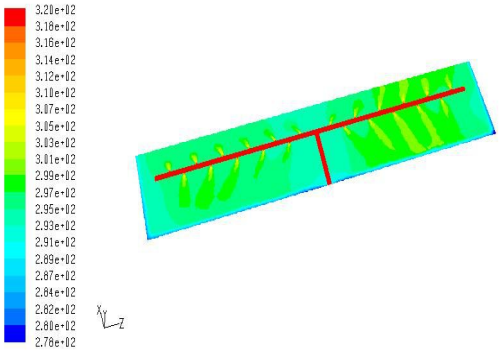

(b)

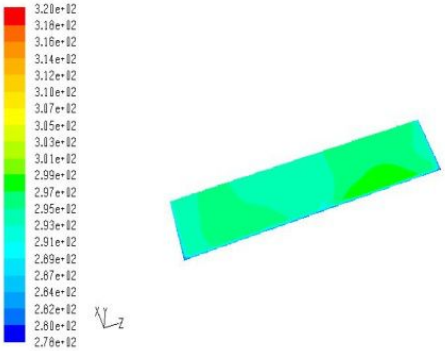

Figure 5. Temperature distribution in different sections. a) Temperature distribution in the section (*Y* = 2.4 m); b) Distribution of crop-canopy temperature in section (*Y* = 1.2 m).

***2. Effect of height of thermal screen*:** In a large glass green house, the heating efficiency is low because warm air is less dense and therefore rises because of the buoyancy effect. To improve the heating efficiency, a thermal screen is usually installed in the green house. Figures 6 (7) show the temperature distribution when a 3.6-m-high (3.0-m-high) thermal screen is installed. As these results show, the ventilation gradually increases along the duct and, because of wind pressure, the warm air diffuses across the width of the green house. Due to the horizontal obstacle that is the thermal screen, neither energy nor mass could be transmitted upward, thus greatly reducing the space available for exchange between warm air and indoor air.

Thus, the airflow patterns change greatly as a result of using the thermal screen. The local airflow under the duct improves significantly, reducing the airflow between the roof and the thermal screen and facilitating the transfer of thermal energy in the space below the thermal screen. Thus, the presence of the thermal screen increases the temperature in the lower space by reducing the volume available for thermal-energy transfer.

As seen from Fig. 6, the temperature ranges from 290.65 to 296.95 K (temperature difference of 6.30 K) at the crop-canopy level when using a 3.6-m-high thermal screen. However, in Fig. 7 the temperature ranges from 292.65 to 300.95 K (temperature difference of 8.30 K) at the crop-canopy level when using a 3-m-high thermal screen. Thus, the temperature difference is larger for lower thermal screens, and the average temperature is higher. However, the proper crop temperature is not exceeded, which means that the green house offers a better growing environment with the lower thermal screen. In addition, for a given temperature, less energy is required when using the lower thermal screen.
The effect of the thermal screen would improve were it positioned above the green house or around the green house. As can be seen from Figs. 6 and 7, a lower thermal screen results in an increased and more uniform temperature, all other things held constant. Although a lower thermal screen leads to improvements, physical constraints such as the height of crops, operators, and other equipment should be considered synthetically.

(a)

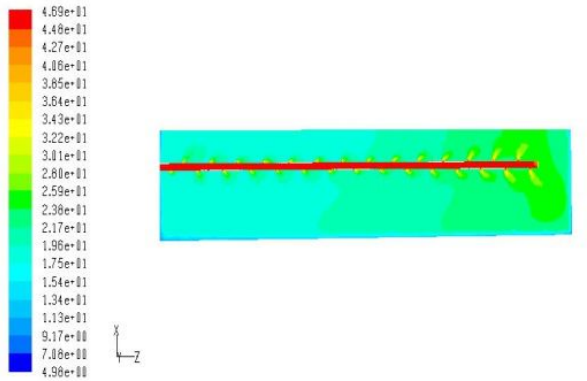

(b)

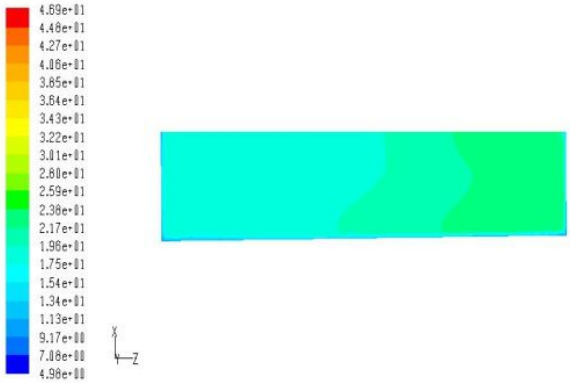

Figure 6. Temperature distribution at different sections of 3.6-m-high thermal screen. a) Temperature distribution in section (*Y* = 2.4 m); b) Distribution of temperature at crop-canopy level in section (*Y* = 1.2 m).

(a)

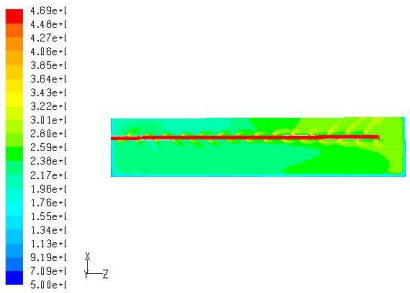

(b)

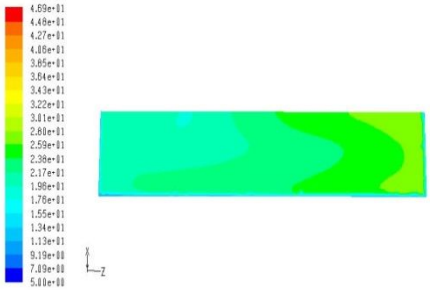

(a) (b)

Figure 7. Temperature distribution in different sections of 3.0-m-high thermal screen. a) Temperature distribution in section (*Y* = 2.4 m); b) Distribution of temperature at crop-canopy level in section (*Y* = 1.2 m).

DISCUSSION

***Simulation of Venlo-type green house*:** The results presented above of the simulation of the temperature distribution inside a Venlo-type green house are consistent with the analytical results reported by Sheng (2007), which indicates that the model presented herein is valid for simulating the temperature distribution in a green house.

***Configuration of warm-air vent*:** Another factor that influences the green house environment is the configuration of the warm-air vent. Of the three cases simulated, the average temperature at the crop-canopy level ranges from 290.15 to 304.75 K, with the highest temperatures occurring in the case of the downward-directed warm-air outlet, followed by the optimized duct (292.55~297.95 K), and finally the horizontally directed warm-air outlet (288.15~296.95 K). For the downward-directed warm-air outlet, warm air diffuses down directly and exchanges more thermal energy with the lower air because of this forced convection. Thus, the temperature of the lower air rises, resulting in a relatively high temperature at the crop level. However, for the other two cases, warm air flows horizontally and exchanges thermal energy with the lower

air only by natural convection, leading to a lower average temperature. The temperature distribution was the most uniform for the optimized duct, which gave a temperature difference of 5.4 K, followed by the horizontally directed warm-air outlet (temperature difference of 8.8 K), and finally by the downward-directed warm-air outlet (temperature difference of 14.6 K). This result is tentatively attributed to the fact that warm air from the optimized duct is evenly distributed on both sides of the duct and the velocity of the warm air from each outlet is nearly identical. Predicting the temperature distribution is complex because it relates to the size of the warm air outlets, the space between outlets, and the positions of the outlets (*Sheng, 2007*). How these various configurations affect the temperature distribution in the crop area and the energy consumption requires further study.

***Thermal screen*:** The thermal screen is another factor that influences the temperature distribution within a green house. To conserve energy and improve efficiency, a thermal screen is usually used during winter in green houses. Because of the partition provided by the thermal screen and the resulting decrease in the volume available for heat exchange between warm air and indoor air, the air temperature under a thermal screen exceeds that elsewhere, all other things being equal. In addition, the temperature of the air under the thermal screen rises as the thermal screen is lowered. Currently, most thermal screens are installed only on top of green houses. If this approach does not result in the proper temperature for plant growth, thermal screens may be placed around green houses. Wu (2010) argued that green houses with thermal screens would be more humid during winter nights. Thus, because a higher relative humidity affects the transpiration rate of plants and promotes plant disease and pests that stunt plant growth, green houses should be frequently dehumidified.

Finally, because forced-air heating is only one of several methods to heat green houses, more research is necessary to further simulate and analyze how different heating methods affect energy consumption and plant growth.

***Conclusion*:** We develop herein a three-dimension numerical CFD model that incorporates different heating parameters to simulate the green house environment. This model was numerically implemented by using Fluent CFD software. The main conclusions are as follows:

1. Using downward-directed warm-air outlets as opposed to horizontally directed warm-air outlets results in a higher average temperature in the green house and lower energy consumption. However, the higher temperature exceeds that required for crop growth, and the temperature distribution at the crop-canopy level is fairly uneven.
2. To reduce the volume available for thermal-energy transfer, a thermal screen is usually used in green houses during the winter. The results of the simulations show that a higher average green house temperature results from using a thermal screen than for no thermal screen. The results of simulations with the thermal screen set at different heights show that a higher average temperature is obtained at the crop-canopy level and less energy is consumed when the thermal screen is set at a lower position.
3. When using a warm-air-delivery duct, the different air velocity from each outlet results in different energy exchange rates in different areas, making it difficult to achieve a uniform temperature distribution. The optimized duct improved this situation: the air velocity at each outlet becomes essentially the same because of the shorter duct, and the temperature distribution becomes more uniform at the crop-canopy level, which is an improvement in terms of both crop growth and energy consumption.

***Acknowledgments*:** The authors are grateful to the National Major Fundamental Research Program of China (Project No. 2005CCA04600), the Major Program of the Science Technology Department of Zhejiang Province (Project No. 20060374), and the Natural Science Foundation of Ningbo City, China (Project No. 2010A610080) for providing the financial support for this research.

REFERENCES

Baille, A., J.C. López, S. Bonachela, M.M. González-Real and J. I. Montero. 2006. Night energy balance in a heated low-cost plastic green house. Agr. Forest Meteorol. 137: 107-118.

Ghosal, M.K. and G.N. Tiwari. 2004. Mathematical modeling for green house heating by using thermal curtain and geothermal energy. Sol. Energy 76: 603-613.

Hoare, E.R. and L.G. Morris. 1956. The heating and ventilation of glasshouses. J. Br. Agric. Eng. XII. 1:1-26.

Kempkes, F.L.K., N.J. Van de Braak and J.C. Bakker. 2000. Effect of heating system position on vertical distribution of crop temperature and transpiration in green house tomatoes. J. Agric. Eng. Res. 75: 57-64.

Meneses, J.F. and A.A. Montero. 1990. Ducted air-heating systems in green houses: experimental results. Acta Hortic. 263: 285-292.

Nachidi, M., F. Rodríguez, F. Tadeo and J.L. Guzman. 2011. Takagi-Sugeno control of nocturnal temperature in green houses using air heating. ISA Trans. 50: 315-320.

Perdigones, A., J.L. García, M. Pastor, R.M. Benavente, L. Luna, C. Chaya and S. de la Plaza. 2006. Effect

of heating control strategies on green house energy efficiency: experimental results and modeling. Trans. ASABE 49: 143-155.

Sethi, V.P. and S.K. Sharma. 2007. green house heating and cooling using aquifer water. Energy 32: 1414-
1421.

Sheng, J.Q. 2007. Numerical analysis of hot-blast heated green house thermal environment. M.S. diss., Dept. Mech. Eng., Zhejiang University of Technology, Hangzhou, China.

Tao, W.Q. 2004. Numerical heat transfer theory. Xi'an Jitong University Press, Xi'an, China.

Teitel, M., I. Segal, A. Shklyar and M. Barak. 1999. A comparison between pipe and air-heating methods for green houses. J. Agric. Eng. Res. 72: 259-273.

Teitel, M. and J. Tanny. 1998. Radiative heat transfer from heating tubes in a green house. J. Agric. Eng. Res. 69: 185-188.

Tong, L., Z. Zhang, Z.G. Chen and T.Z. Zhang. 2003. Simulation of mechanical ventilation for
Huabei-type multi-span plastic green house. J. Chin. Agric. Univ. 8: 33-37.

Wang, F.J. 2004. Computational fluid dynamic analysis-CFD software theory and application. Tsinghua Press, Tsinghua, China.

Wu, F.Q. 2011. Numerical simulation on thermal environment of heated glass green house based on porous medium. Trans. CSAM 42: 180-185.

Wu, F.Q., L.B. Zhang, F. Xu and J.L. Chen. 2010. Numerical simulation of the thermal environment in a mechanically ventilated green house. Trans. CSAM 41: 153-158.

Wang, J.Q. and B.L. Zhang. 2006. Application of some cooling measures for green house cooling in summer. Trans. CSAE 22: 257-260.

Willits, D.H. and Y. R. Gurjer. 2004. Heat pumps for the heating and night-cooling green house crops: a simulation study. Trans. ASAE 47: 575-584.

Zhu, W.J. 2005. CFD Simulation of the heat environment of multi-span green house at night in winter under heating. M.S. diss., Dept. Water Resources and Civil Engineering, Chinese Agricultural University, Beijing, China.

$$\frac{dI(\vec{r},\vec{s})}{ds}+(a+\sigma_s)I(\vec{r},\vec{s})=$$

$$an^2\frac{\sigma T^4}{\pi}+\frac{\sigma_s}{4\pi}\int_0^{4\pi}I(\vec{r},\vec{s}')\Phi(\vec{s},\vec{s}')d\Omega' \quad \vec{r}\ \vec{s}\ \vec{s}'\ s\ a\ n\ \sigma_s$$

$$\sigma\ I\ \vec{r}\ \vec{s}\ T\ \Phi\ \Omega' \quad (a+\sigma_s)s\ n \quad S_{\varphi 2}=Q_{\text{sen}}+Q_{\text{lat}} \quad S_{\phi 2}\ Q_{\text{sen}}$$

$$Q_{\text{lat}} \quad Q_{\text{sen}}=2I_{\text{LA}}\rho C_p(T_c-T_i)/r_a \quad I_{\text{LA}} \quad C_p \quad T_c \quad T_i \quad r_a$$

$$r_a=840\left(d/|T_c-T_i|\right)^{0.25} \qquad r_a=220\left(d^{0.2}/u^{0.8}\right)$$

$$Q_{\text{lat}}=I_{\text{LA}}\rho\lambda_1\left(H_c-H_a\right)/\left(r_a+r_s\right), \quad \lambda_1 \quad H_c \quad H_a \quad r_s$$

$$r_s=200\left[1+e^{0.05(R_{\text{gi}}-50)}\right]\left[1+0.11e^{(0.34D_i/100-10)}\right] \quad (\rho)\ (\lambda)\ (\beta)\ \mu\ (\rho)\ v$$

$$\oint\rho\phi\,\vec{v}\cdot d\,\vec{A}=\oint\Gamma_\phi\nabla\phi\cdot d\,\vec{A}+\int_V S_\phi dV \quad \rho$$